Journal of Crystal Growth 405 (2014) 52–58

Contents lists available at ScienceDirect

Journal of Crystal Growth

journal homepage: www.elsevier.com/locate/jcrysgro

Influence of temperature-dependent thermophysical properties of sapphire on the modeling of Kyropoulos cooling process

Z.L. Jin [a], H.S. Fang [a,*], N. Yang [a], Z. Zhang [a], S. Wang [a], J.F. Xu [b,**]

[a] School of Energy and Power Engineering, Huazhong University of Science and Technology, Wuhan 430074, China
[b] School of Mechanical Science and Engineering, Huazhong University of Science and Technology, Wuhan 430074, China

ARTICLE INFO

Article history:
Received 9 January 2014
Received in revised form
13 May 2014
Accepted 28 July 2014
Communicated by: A.G. Ostrogorsky
Available online 5 August 2014

Keywords:
A1.Thermophysical properties
A1. Numerical simulation
A2. Kyropoulos
B1. Sapphire

ABSTRACT

Sapphire is widely used as substrates in semiconductor industry. Kyropoulos (Ky) method is the most popular technique to grow large-size and substrate-quality sapphire single crystals. Computational modeling is a powerful tool to analyze the growth conditions for the improvement of this crystal growth. for simulation, thermophysical properties of sapphire are usually set constant, which may increase the deviation between experiments and modeling results. In this paper, temperature-dependent properties of sapphire, i.e., heat capacity, thermal conductivity, and thermal expansion coefficient, are summarized and adopted in the simulation studies. Their effects on the predicted results are discussed for the cooling process, during which large temperature change in the crystal leads to big differences of the material properties. Comparative analysis tells that temperature difference and thermal stress can be more than 200 K and 4 MPa for the cases with or without consideration of the temperature-dependence of the properties. Consequently, it is necessary to consider the impact of material properties on the accuracy of numerical simulation during the sapphire single crystal growth.

1. Introduction

Sapphire is a kind of hexagonal single crystal with excellently physical, mechanical and optical properties [1]. It is widely used in the applications of silicon-on sapphire (SoS) RF devices, coating surfaces, optical windows [2], nuclear track detectors [3], and optical data storages [4]. The recent booming of sapphire is stimulated by its substrate application in high-brightness light emitting diode(LED) industry [1]. Since the first introduction of manual growth [5], technologies of sapphire crystal growth have achieved much progress. This makes it possible to grow high-quality and massive crystals in industry [6]. Several popular methods have been employed in industry to grow large sapphire ingots, for example, Czochralski (Cz), Ky, Heat exchanger method (HEM), and Stepanov method (EFG), among which Ky is the most widely used method for its advantages of relatively low cost and high crystal quality. However, lack of comprehensive understanding of the growth process is impeditive to optimize the growth parameters for further improvement of the crystal quality and productivity. Theoretical analysis only provides qualitative explanation for growth process on account of the complex differential equations and intricate boundary conditions. Experimental studies not only disturb the normal growth conditions, but also are significantly limited by the specific growth environment, such as high system temperature. High cost and low efficiency of a real production experimental study further prevent the industry to perform accurate measurements of temperature, velocity and stress distributions [7] during growth and modify growth parameters and system structures. Computational calculations, otherwise, work as a replacement of the experimental studies for a detailed investigation of the growth process with absolute advantages in time and cost.

High-quality sapphire is characterized by low thermal stress-induced defects, for example, dislocation, bubbles and cracks. Although Ky method distinguishes itself from other techniques in low temperature gradients during growth, defects such as dislocation keeps a major challenging issue affecting crystal quality. In the past years, Ky-growth of sapphire crystal has been widely investigated numerically [8–10]. Demina et al. [11] compared two designs of the furnace with consideration of radiation heat transfer and melt convection, and obtained the preferred furnace structure. Chen et al. [12] performed simulation analysis of temperature and velocity distributions in the crucible for different growth stages to show the dominant characteristics. Lee et al. [13] studied effects of crucible geometry on the convexity of the liquid/solid interface, and concluded that curved crucible bottom is

* Corresponding author. Tel.: +86 27 87542618.
** Corresponding author.
E-mail addresses: hafang@gmail.com (H.S. Fang), jfxu@hust.edu.cn (J.F. Xu).

http://dx.doi.org/10.1016/j.jcrysgro.2014.07.049
0022-0248/

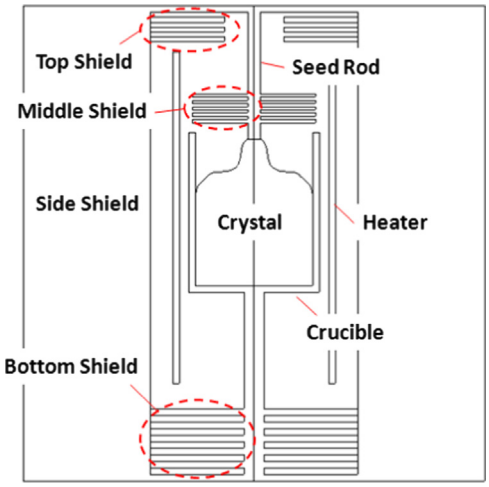

Fig. 1. Schematic structure of Ky furnace.

beneficial for growth. From these studies, we can get much knowledge of Ky growth process regarding heat transfer and fluid flows for possibly improvement of sapphire quality. Although successful agreements are achieved with experiments, one of the major shortcomings in these studies is use of constant thermophysical properties of sapphire. During the entire growth process, especially cooling stage, the system has a large temperature variation, and the assumption of constant properties undoubtedly aggravates the deviation of simulation results from the experimental measurements. In this paper, we summarize several thermophysical properties of sapphire in a wide temperature range, from room temperature to near melting point, and adopt them in the simulation of cooling process during sapphire growth. Comparison of simulation results indicates that to achieve reasonable and quantitative results, the variation of thermophysical properties of sapphire must be taken into account in modeling.

2. Problem description and mathematical models

A schematic structure of Ky furnace used in the present study is shown in Fig. 1. Raw materials are loaded into an iridium crucible, which is supported by a molybdenum rod. The rod above the crucible is used to hold the crystal seed at seeding stage. Three groups of heat shields, namely, the top shield, the side shield and the bottom shield, are arranged in furnace satisfying the hot zone requirement. These heat shields are made of parallel plates of molybdenum. A tungsten heater is used as the resistive heating source. The shields and other insulation parts enclose the growth furnace to prevent heat loss. In the current study, to notably reflect the effect of temperature-dependence of thermophysical properties, the unsteady cooling stage with large temperature change in the crystal is examined.

During the cooling stage, the heater power decreases gradually in a linear mode, and initiates when the melt has been solidified completely. The furnace is vacuumed during the growth and cooling stage, so only conduction and radiation heat transfers exist in the furnace. The space inside the chamber is transparent, while the solids are all treated as opaque, including sapphire ingot regardless of the fact that sapphire has definite refractions in some bands [14]. The influence of such an approximation on heat transfer is compensated by the treatment of internal radiation inside sapphire. To relieve calculation loads as well as to focus on the effects of material properties, internal radiation inner the crystal is evaluated by an effective thermal conductivity. The outer walls of furnace are cooled by room air, and this remains the walls almost at room temperature. The seed rod in furnace is cooled by water, and hence the rod tip is at low temperature location in the furnace as a hot sink during the growth [11].

Temperature-dependent values of heat capacity, thermal expansion and thermal conductivity are employed in simulation. The cooling process starts from a high system temperature close to the melting point of sapphire, and lasts about 40 h. The heating power linearly reduces from an initial value to zero during the process. The fundamental equations are listed in the following.

Energy equation in the heater:

$$\rho C_h \frac{\partial T_h}{\partial t} = \nabla \cdot (\kappa_h \nabla T_h) + Q, \tag{1}$$

Energy equation in the crucible, insulators, rods, shields, and sapphire:

$$\rho C_i \frac{\partial T_i}{\partial t} = \nabla \cdot (\kappa_i \nabla T_i), \tag{2}$$

Energy balance at the solid/vacuum interface:

$$-\kappa_i \frac{\partial T_i}{\partial \hat{n}} = \sigma_B \varepsilon_i (T_i^4 - T_{a,i}^4), \tag{3}$$

where T_i is temperature, and κ_i is thermal conductivities of the furnace components, which is an effective value in sapphire; the subscript i indicates the components of the furnace, i.e., crucible, shields and sapphire ingot. Q is the heat source, σ_B is the Stefan-Boltzmann constant, and $\hat{n}$ is the unit normal vector. $T_{a,i}$ is the environment temperature for radiation heat transfer, which is calculated by [12]

$$T_{a,i} = \left(\frac{1}{\varepsilon_i A_i} \sum_{j=1}^{N} X_{ij} \varepsilon_j A_j T_j^4 \right)^{1/4}, \tag{4}$$

where ε, A, and X_{ij} are the emissivity, area, and view factor from area j to area i, respectively. The axisymmetric thermal strain–stress equations for sapphire are calculated in cylindrical coordinate [12]. Thermal elastic stress–strain relation is based on Hooke's law,

$$\sigma = C : (\varepsilon_0 - \alpha(T - T_{ref})), \tag{5}$$

where α is the thermal expansion coefficient, and C is the elastic constant matrix given as

$$C = \frac{E}{(1+\nu)(1-2\nu)} \begin{bmatrix} 1-\nu & \nu & \nu & 0 \\ \nu & 1-\nu & \nu & 0 \\ \nu & \nu & 1-\nu & 0 \\ 0 & 0 & 0 & 1-\nu \end{bmatrix}, \tag{6}$$

where E is the elastic modulus, and ν is the Poisson's ratio. The stress distribution in sapphire ingot is calculated with a fixed boundary condition on the crucible walls where the crystal contacts. To calculate stress distribution, the following equations are solved,

$$\frac{1}{r}\frac{\partial (r\sigma_{rr})}{\partial r} + \frac{\partial (\sigma_{rz})}{\partial z} - \frac{\sigma_{\varphi\varphi}}{r} = 0, \tag{7}$$

$$\frac{1}{r}\frac{\partial (r\sigma_{rz})}{\partial r} + \frac{\partial (\sigma_{zz})}{\partial z} = 0, \tag{8}$$

where σ_{rr}, σ_{zz} and $\sigma_{\varphi\varphi}$ are the three normal stresses in cylindrical coordinate, and σ_{rz} is the shear stress. The von Mises stress is calculated to evaluate the stress level during crystal cooling, which can be expressed as

$$\sigma_M = \sqrt{\frac{(\sigma_{rr} - \sigma_{zz})^2 + (\sigma_{rr} - \sigma_{\varphi\varphi})^2 + (\sigma_{zz} - \sigma_{\varphi\varphi}) + 6\sigma_{rz}^2}{2}} \tag{9}$$

3. Results and discussion

3.1. Thermophysical properties of sapphire

Thermophysical properties of sapphire vary significantly by temperature; however, as aforementioned, they are often assumed as constants during numerical simulation [9–13,15–18] according to the values measured at room temperature or at the melting point. The most important properties are thermal capacity, thermal conductivity and thermal expansion in a unsteady calculation. In the current reports, the three major thermophysical properties are investigated comprehensively, while other properties, such as the elastic modulus and Poisson's ratio are still assumed temperature-independent as shown in Table 1.

As mentioned previously, sapphire is treated as opaque with an effective thermal conductivity to consider internal radiation. Such a treatment remains the semi-transparent radiation features in sapphire with a significant relief of the computational load by avoiding direct calculation of the radiative heat transfer equations. The Rosseland approximation is utilized to determine the effective thermal conductivity [10,19],

$$\kappa = \kappa^{\mathrm{mod}} + \kappa^{rad} = \kappa^{\mathrm{mod}} + \frac{16n^2\sigma_B T^3}{3\alpha_R}, \tag{10}$$

where κ^{mod} is the general thermal conductivity, and κ^{rad} is the effective thermal conductivity considering radiation heat transfer. The parameters, n and α_R, are the refractive index and the Rosseland mean absorption coefficient, respectively. The effective thermal conductivity is shown in Fig. 2a, which is proportional to the third order of temperature. As the temperature reaches 2300 K, the effective thermal conductivity is more than 600 W/m-K much higher than the original molecular thermal conductivity [12]. The nominal total thermal conductivity is also shown in Fig. 2a. The value is much larger than the widely used value of 17.5 W/m-K [20,21] or 5.8 W/m-K [11], 5 W/m-K[13] and 3.5 W/m-K [12] in the previous publications. One can further find that as the temperature goes up, the contribution of radiation becomes more important for heat conduction.

Thermal expansion coefficient critically influences the calculation of thermal stress field. Since sapphire is often used as the reference material to measure thermal expansion coefficients of other materials, its expansion coefficient has been well studied by many researchers. However, in sapphire growth simulation, this variable is still simplified as a constant value of $1.8\times10^{-5}\mathrm{K}^{-1}$ [12,13,20] or $5.0\times10^{-6}\mathrm{K}^{-1}$ [16]. Indeed, it is highly temperature-dependent. Harris [22] proposed a formula to describe it as

$$\alpha = X + Y\cdot T - Z\cdot\exp[-W\cdot(T-273)], \tag{11}$$

where X, Y, Z and W are constants taken as 8.026×10^{-6}, 8.17×10^{-10}, 3.27×10^{-6} and 3.279×10^{-6}, respectively. This expression has been used by Chen et al. in their study [9]. A curve to visualize this formula is shown in Fig. 2b. The values from the handbook of sapphire perpendicular to c-Axis of sapphire [14], from Ref. [23], and from Ref. [24] are also drawn in the figure. The differences of these datas may result from the measurement techniques and the sample quality. The datas presented by Fiquet et al. [24] are based on adequate experiments, so it is possible more reasonable. The least-square fitted expression of the datas are expressed as

$$\alpha = \alpha_0 + \alpha_1 T + \alpha_2/T^2, \tag{12}$$

Table 1
Material properties of sapphire used in calculations.

Physical property	Value
Density ρ_C(kg/m^3)	3960
Molecular thermal conductivity κ^{mol}(W/m-K)	17.5
Heat capacity C (J/kg-K)	1430
Thermal expansion coefficient α(1/K)	1.8×10^{-5}
Emissivity ε	0.9
Refractive index n	1.78
Absorption coefficient α_R(m^{-1})	19.26
Stefan–Boltzmann constant σ_B(W/m^2-K^4)	5.67×10^{-8}
Elastic modulus E (Pa)	3.45×10^{11}
Poisson's ratio ν	0.28

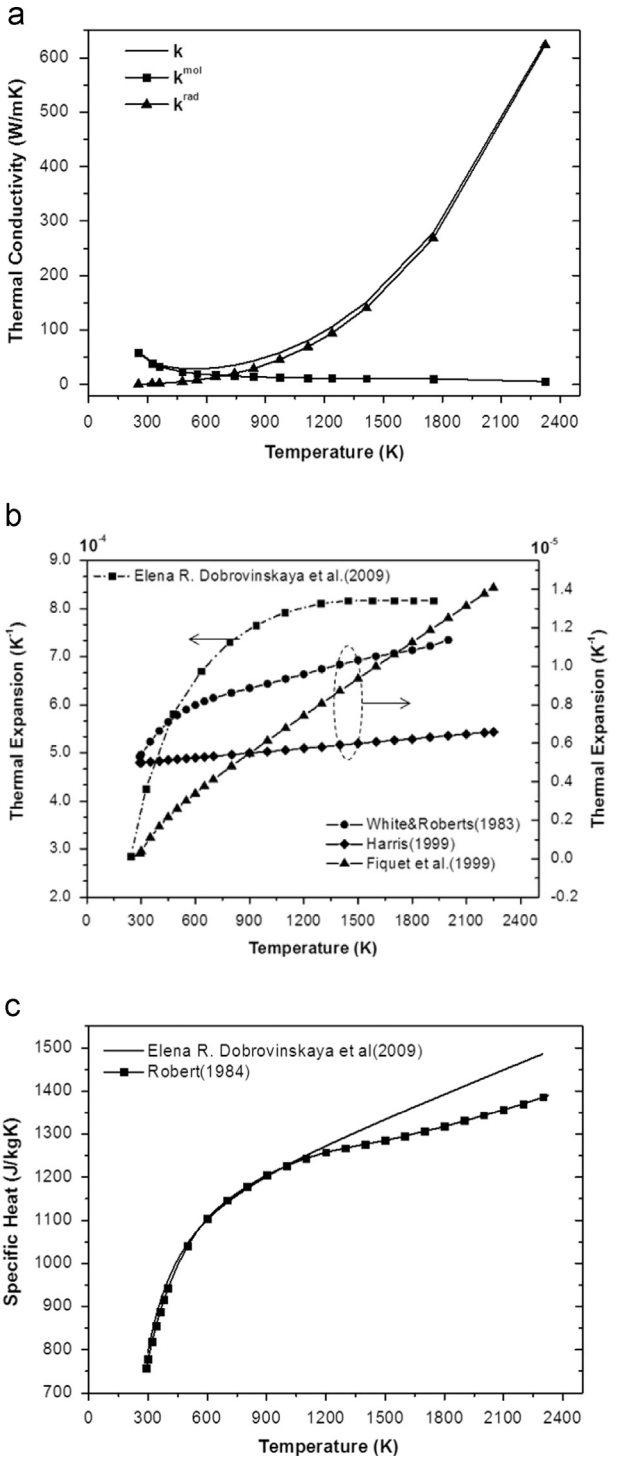

Fig. 2. (a) The effective thermal conductivity predicted by Rosseland model, (b) thermal expansion coefficient as a function of temperature, and (c) variation of heat capacity by temperature.

where α_0, α_1 and α_2 are 2.137×10^{-5}, 0.627×10^{-8}, and -0.134, respectively. The thermal expansion coefficient curves in Fig. 2b obviously show the differences between the values, which is also noted by Fiquet et al. [24]. In this paper, we adopted the expression of Eq. (12) to calculate thermal expansion coefficient of sapphire.

The specific heat of sapphire is also highly temperature-dependent. In previous studies, the heat capacity of sapphire is often set as a constant of 765 J/kg-K [9,12,20,21,25] or 1430 J/kg-K [13,16] regardless of the fact that its relation to temperature has been presented [14],

$$C_p = 4.2\times(26.12+4.388\times10^{-3}T-7.269\times10^{5}T^{-2}) \quad (13)$$

The curve of formula for Eq. (13) is shown in Fig. 2c. Robert [26] reviewed many previous studies, and recommended a more reliable expression,

$$C_p = A_1T^{-4}+A_2T^{-3}+A_3T^{-2}+A_4T^{-1}+A_5+A_6T+A_7T^2+A_8T^3+A_9T^4. \quad (14)$$

The parameters, A_n ($n=1\sim9$), vary by temperature, and can be found in Ref. [26]. Eq. (14) is adopted in current study, and the curve is presented in Fig. 2c.

3.2. Effect of thermophysical properties

The constant properties are first used in simulation as a reference, and then the temperature-dependent properties are adopted for further comparison studies. The initial values for time-dependent calculations of cooling process are from the convergent steady solutions with the power consumption at the beginning of cooling. Temperature and stress distributions with constant properties are shown in Fig. 3a. From left part of the figure, one can see that the crucible and crystal are in high temperature, and the seed rod has a low temperature due to water-cooling. Large temperature gradients exist in the crucible. Distribution of von Mises stress inside the crystal is depicted at the right part of the figure. Three monitoring points, A, B and C as marked in the figure, are selected for further analysis. Point A is located inner the crystal, and Point B and Point C are along the symmetric axis. The variables written as $P(v)$ represent that the field P is obtained when the property v is temperature-dependent in the simulation. For example, $T(\kappa)$ denotes temperature field achieved when thermal conductivityκchanges by temperature. A linear power change profile is applied during the cooling as shown in Fig. 3b.

Fig. 4 shows temperature and stress evolutions at Points A, B and C during the whole cooling time. These curves tell that all cases have the same tendencies of temperature and stress evolutions. With the linear ramp-down of heat power, temperature distribution in furnace goes down continuously, which is reflected by the two sets of temperature profiles at the three points in Fig. 4. The upper set of the curve is composed of three curves respective to T, $T(C)$ and $T(\alpha)$. When the constant properties, or temperature-dependent heat capacity, or temperature-dependent thermal expansion coefficient are applied, temperature changes at the three points are very close during the entire cooling process. The lower set includes two curves. One is with temperature-dependent thermal conductivity $T(\kappa)$, and the other considers variations of all the listed thermophysical properties by temperature $T(C,\kappa,\alpha)$. It is noted that the maximum temperature difference with or without consideration of temperature-dependent properties can be up to 200 K at the cooling stage in Fig. 4. The curves also tell that specific heat and thermal expansion coefficient have less impact on the temperature field. However, thermal conductivity value leads to much difference of temperature predictions. The stress curves have different characteristics comparing

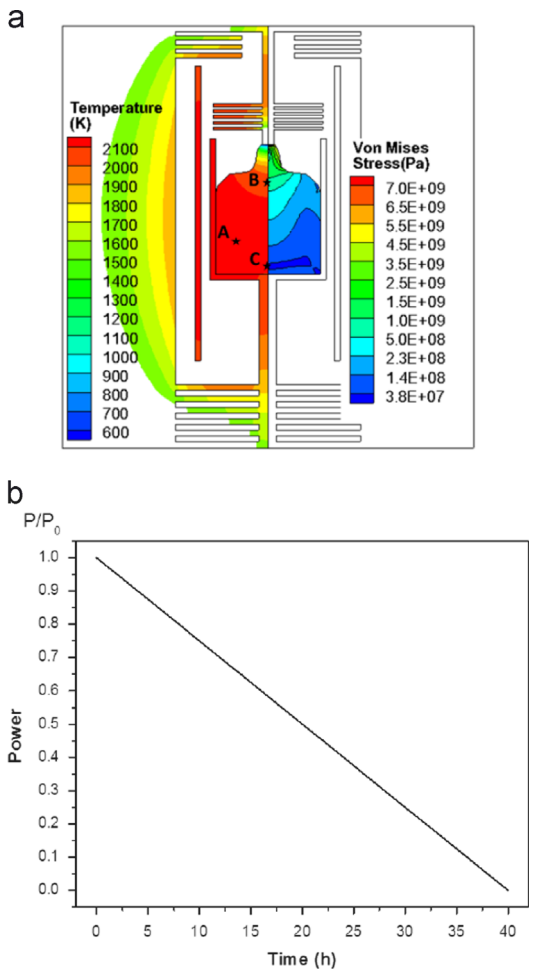

Fig. 3. (a) Temperature and stress distributions at the staring cooling of sapphire growth with constant properties, and (b) the linear power ramp-down profile for the cooling stage used in the simulation.

to temperature profiles. The von Mises stress in crystal decreases as the cooling proceeds. The case only taking into account of thermal expansion coefficient $\sigma(\alpha)$ has the largest stress about 10.5 MPa at the early cooling, while the case of $\sigma(\kappa)$ shows the lowest value about 6.7 MPa. It is noticeable that besides a slight difference at the starting cooling, the curves of σ and $\sigma(C)$ are almost overlapped, which states that specific heat influences stress field ineffectively. Comparing to the case with a complete consideration of listed properties, $\sigma(C,\kappa,\alpha)$, only treatment of the thermal conductivity $\sigma(\kappa)$ results in an underestimation of stress level at early cooling stage, and leads to an overestimation at late stage. In Addition, one can find that constant properties, overall, make the simulation results overestimated after a certain cooling time. However, stress levels of Point C at early cooling stage with a complete consideration of the properties are much larger than those of others. It emphasizes that the effect of thermophysical properties on the predicted results also depends on local growth conditions. From above analysis, one can know that the impact of temperature-dependent properties should be carefully examined in the modeling. In addition, the overlapped lines show that the temperature varied specific heat has not much impaction on the results. The reason is that the released/absorbed heat of sapphire with temperature change is small compared to the total heat flux.

Contours of temperature and stress distributions are also presented for comparison analysis. Figs. 5 and 6 give temperature distributions in the right and von Mises stress distributions in the left at cooling time 15 h and 25 h, respectively. From the Figures,

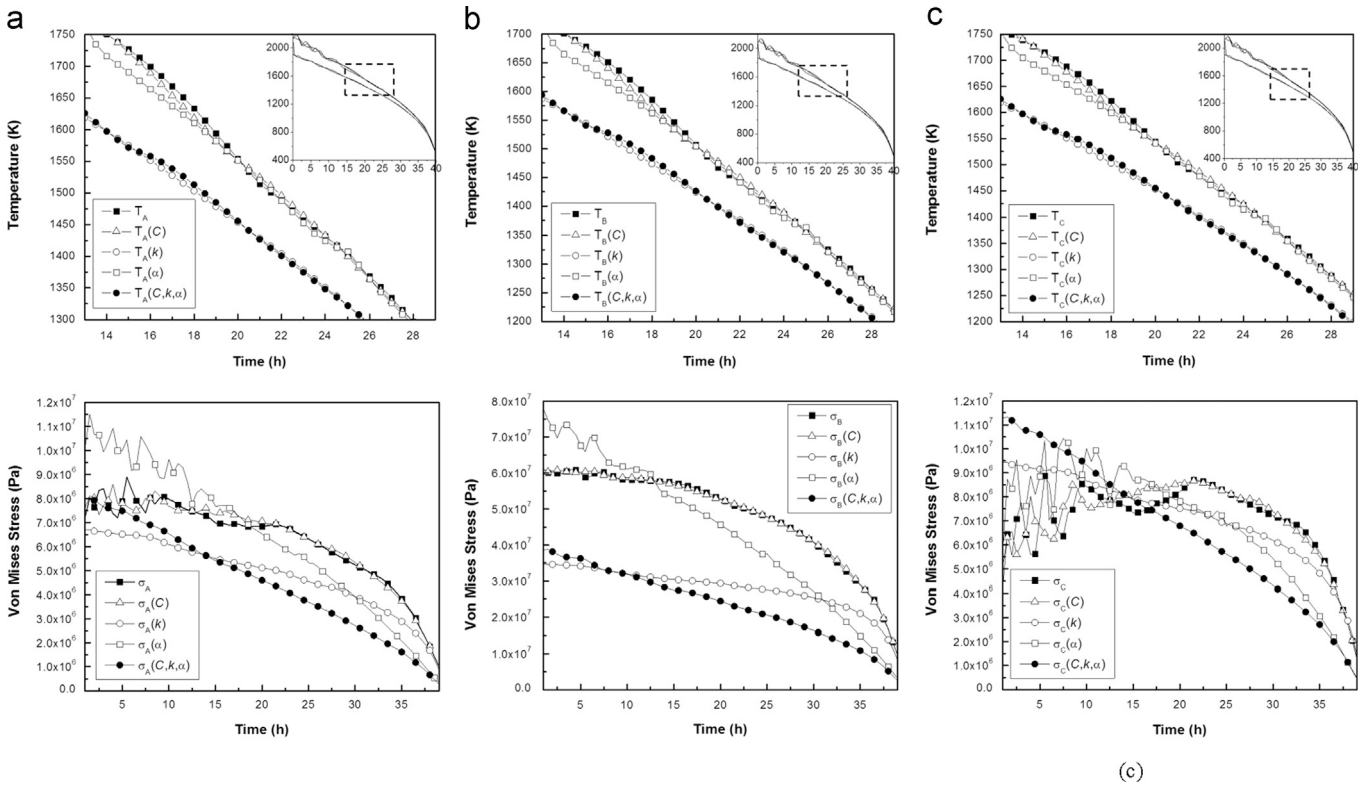

Fig. 4. The temperature and stress changes during the cooling (a) at Point A, (b) at Point B, and (c) at Point C.

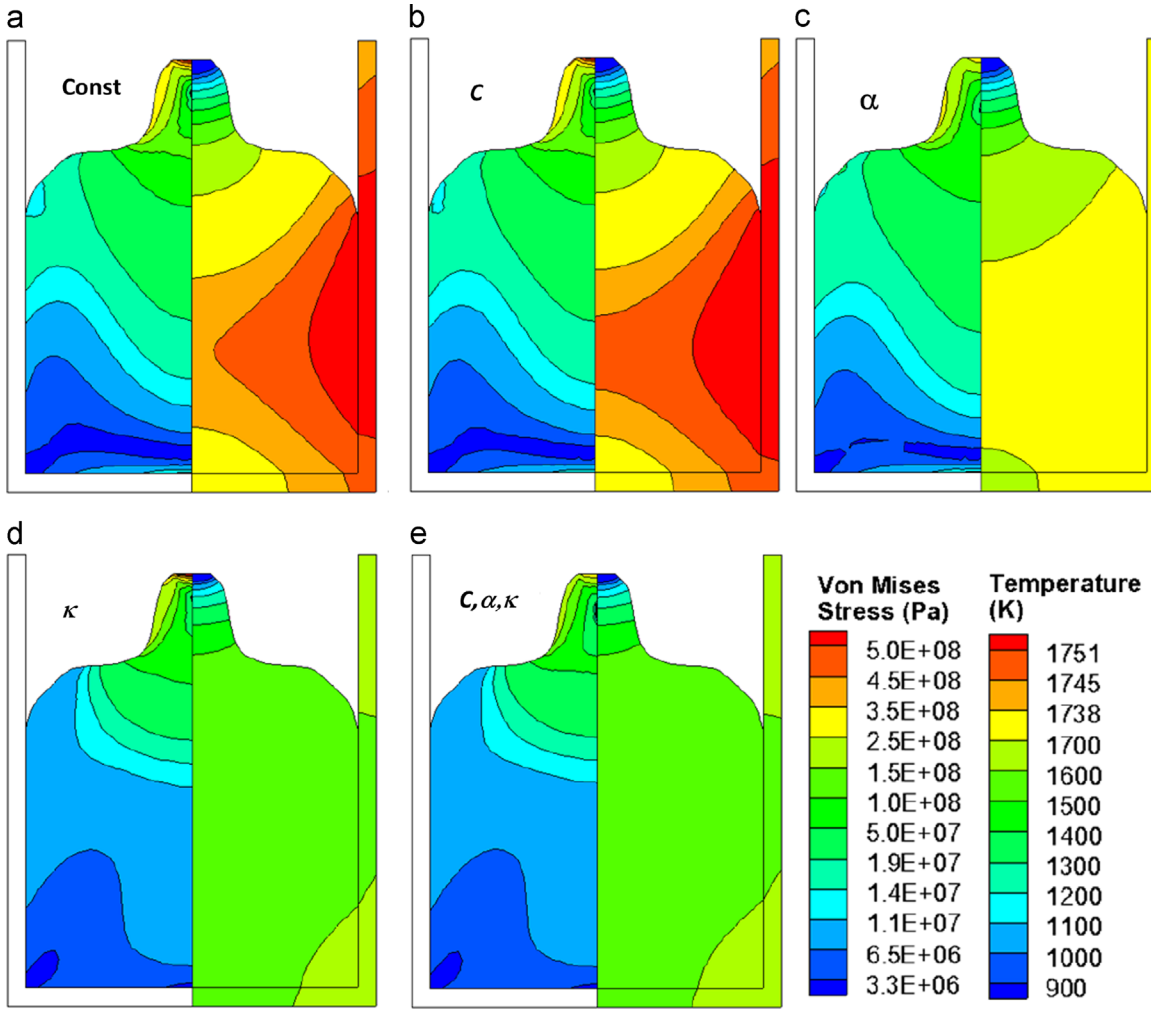

Fig. 5. von Mises stress (left part) and temperature (right part) distributions at the cooling time of 15 h with (a) the constant properties, (b) temperature-dependent heat capacity, (c) temperature-dependent thermal expansion coefficient, (d) temperature-dependent thermal conductivity, and (e) full consideration of the listed properties.

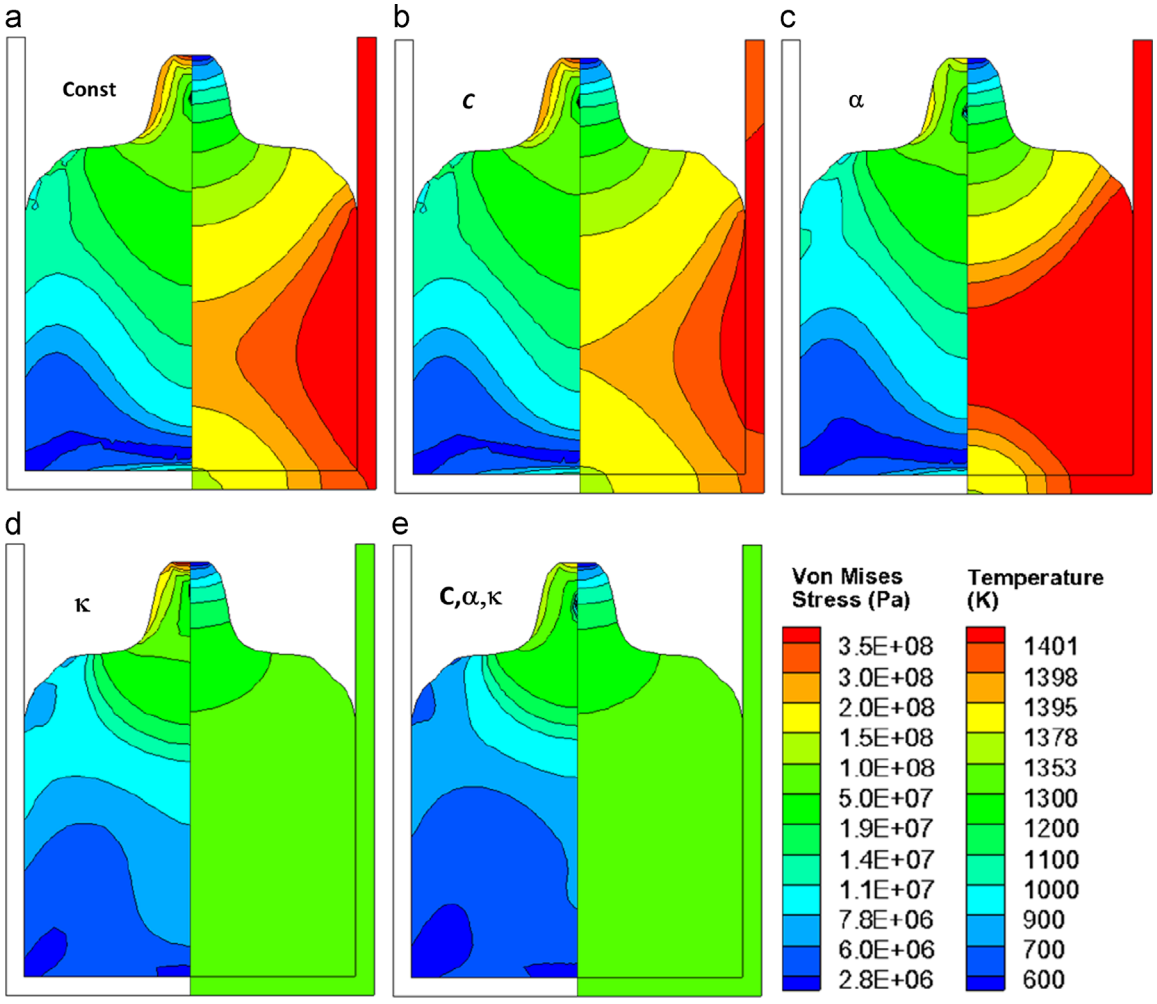

Fig. 6. von Mises stress (left part) and temperature (right part) distributions at the cooling time of 25 h with (a) the constant properties, (b) temperature-dependent heat capacity, (c) temperature-dependent thermal expansion coefficient, (d) temperature-dependent thermal conductivity, and (e) full consideration of the listed properties.

one can know that high temperature zone with constant properties is larger than that of other cases. So is the case with temperature-dependent heat capacity. The result is consistent with the temperature profile in Fig. 4. Despite the difference of temperature patterns, the stress patterns at both cooling times are similar when constant properties, temperature-dependent specific heat and temperature-dependent thermal expansion coefficient are used. When temperature-dependent thermal conductivity is considered (Figs. 5d, 4e, 6d and e), more uniform stress distributions in the crystal are obtained.

4. Conclusions

In the paper, numerical simulation has been performed to analyze heat transfer and thermal stress during the cooling of Ky-sapphire growth. Effects of temperature-dependent thermophysical properties of sapphire have been investigated. It is found that specific heat will not cause significant difference for the simulation results of temperature and stress distribution. Thermal conductivity must be considered with temperature-dependent for a reasonable prediction of temperature and thermal stress distributions. Furthermore, thermal expansion coefficient has a strong impact on thermal stress field. The maximum deviations of temperature and stress are up to about 200 K and about 4 MPa, respectively, without proper applications of the thermophysical properties. Therefore, it is necessary to consider the variations of sapphire properties by temperature for a quantitatively numerical analysis.

Acknowledgments

The work is supported in part by the National Natural Science Foundation of China (NSFC51106059), and is also supported in part by Key Foundation of Hubei Province (2013CFA080).

References

[1] M.S. Akselrod, F.J. Bruni, Modern trends in crystal growth and new applications of sapphire, J. Cryst. Growth 360 (2012) 134–145.
[2] Hongbo Zuo Guigen Wang, Huayu Zhang, Qibao Wu, Mingfu Zhang, Xiaodong He, Zhaohui Hu, L.i.n. Zhu, Preparation, quality characterization, service performance evaluation and its modification of sapphire crystal for optical window and dome application, Mater. Des. 31 (2010) 706–711.
[3] G.M. Akselrod, M.S. Akselrod, E.R. Benton, N. Yasuda, A novel Al_2O_3 fluorescent nuclear track detector for heavy charged particles and neutrons, Nucl. Instrum. Method B 247 (2006) 295–306.
[4] Mark Akselrod, Aluminum oxide material for optical data storage, in, Google Patents, 2005.
[5] K. Nassau Dr, AVL, Verneuil: the man and the method, J. Cryst. Growth 13 (1972) 12–18.
[6] Daniel C Harris, in: Proceedings of the 10th DoD Electromagnetic Windows Symposium. Norfolk, Virginia, A century of sapphire crystal growth, DTIC Document. , 2004.
[7] A.J. Goza, S.E. Tritchler, D.F. Bliss, B.C. Houchens, Thermodynamic modeling of bulk ternary alloy crystal growth: comparison of experiments and theory for GaInSb alloys, J. Cryst. Growth 337 (2011) 60–64.

[8] Xiaoping Su Jinquan Li, Mujilatu Na, Hai Yang, Jianmin Li, Yunqi Yu, Jianjun Mi, Influence of gas flow on thermal field and stress during growth of sapphire single crystal using Kyropoulos method, Rare Met. 25 (2006) 260–266.
[9] Jyh-Chen Chen Chun-Hung Chen, Yi-Shiuan Chiue, Ching-Hsin Chang, Che-Ming Liu, Chi-Yung Chen, Thermal and stress distributions in larger sapphire crystals during the cooling process in a Kyropoulos furnace, J. Cryst. Growth 385 (2013) 55–60.
[10] H.S. Fang, Y.Y. Pan, L.L. Zheng, Q.J. Zhang, S. Wang, Z.L. Jin, To investigate interface shape and thermal stress during sapphire single crystal growth by the Cz method, J. Cryst. Growth 363 (2013) 25–32.
[11] S.E. Demina, E.N. Bystrova, M.A. Lukanina, V.M. Mamedov, V.S. Yuferev, E. V. Eskov, M.V. Nikolenko, V.S. Postolov, V.V. Kalaev, Numerical analysis of sapphire crystal growth by the Kyropoulos technique, Opt. Mater. 30 (2007) 62–65.
[12] Jyh-Chen Chen Chun-Hung Chen, Chung-Wei Lu, Che-Ming Liu, Numerical simulation of heat and fluid flows for sapphire single crystal growth by the Kyropoulos method, J. Cryst. Growth 318 (2011) 162–167.
[13] W.J. Lee, Y.C. Lee, H.H. Jo, Y.H. Park, Effect of crucible geometry on melt convection and interface shape during Kyropoulos growth of sapphire single crystal, J. Cryst. Growth 324 (2011) 248–254.
[14] E.R. Dobrovinskaëïìà, Leonid A Lytvynov, V.V. Pishchik, Sapphire: Material, Manufacturing, Applications, Springer, US (2009) 55–176.
[15] M.H. Tavakoli, H. Wilke, N. Crnogorac, Influence of the crucible bottom shape on the heat transport and fluid flow during the seeding process of oxide Czochralski crystal growth, Cryst. Res. Technol. 42 (2007) 1252–1258.
[16] S.E. Demina, E.N. Bystrova, V.S. Postolov, E.V. Eskov, M.V. Nikolenko, D.A. Marshanin, V.S. Yuferev, V.V. Kalaev, Use of numerical simulation for growing high-quality sapphire crystals by the Kyropoulos method, J. Cryst. Growth 310 (2008) 1443–1447.
[17] C.W. Lu, J.C. Chen, C.H. Chen, C.H. Chen, W.C. Hsu, C.M. Liu, Effects of RF coil position on the transport processes during the stages of sapphire Czochralski crystal growth, J. Cryst. Growth 312 (2010) 1074–1079.
[18] M.H. Tavakoli, Numerical study of heat transport and fluid flow of melt and gas during the seeding process of sapphire Czochralski crystal growth, Cryst. Growth Des. 7 (2007) 644–651.
[19] Irina Nicoara Daniel Vizman, Dumitru Nicoara, On the factors affecting the isotherm shape during Bridgman growth of semi-transparent crystals, J. Cryst. Growth 169 (1996) 161–169.
[20] Jyh-Chen Chen Chung-Wei Lu, Chien-Hung Chen, Chun-Hung Chen, Wen-Ching Hsu, Che-Ming Liu, Effects of RF coil position on the transport processes during the stages of sapphire Czochralski crystal growth, J. Cryst. Growth 312 (2010) 1074–1079.
[21] Jyh-Chen Chen Chung-Wei Lu, Numerical simulation of thermal and mass transport during Czochralski crystal growth of sapphire, Cryst. Res. Technol. 45 (2010) 371–379.
[22] C. Daniel, Harris, Materials for Infrared Windows and Domes, SPIE press, 1999.
[23] G.K. White, R.B. Roberts, Thermal expansion of reference materials: tungsten and $\alpha-$ Al_2O_3, High Temp. High Press. 15 (1983) 321–328.
[24] G. Fiquet, P. Richet, G. Montagnac, High-temperature thermal expansion of lime, periclase, corundum and spinel, Phys. Chem. Miner. 27 (1999) 103–111.
[25] Jyh-Chen Chen Chun-Hung Chen, Chung-Wei Lu, Che-Ming Liu, Effect of power arrangement on the crystal shape during the Kyropoulos sapphire crystal growth process, J. Cryst. Growth 352 (2012) 9–15.
[26] Robert Castanet, Selected data on the thermodynamic properties of α-alumina, High Temperatures High Press. 15 (1984) 449–457.